CO8-1

Detection experiment for nuclear materials positioned away from center

M. Komeda[1], K. Tanabe[2], Y. Toh[1], Y. Kitamura[3], Y. Takahashi[3] and T. Misawa[3]

[1]*Nuclear Science and Engineering Center, Japan Atomic Energy Agency*
[2]*National Research Institute of Police Science*
[3]*Institute for Integrated Radiation and Nuclear Science, Kyoto University*

INTRODUCTION: We have developed a new nuclear material detection method, called the active rotation method, using a neutron rotation machine that rotates a neutron source (Californium-252) at a speed of thousands of rpm. In addition to the rotation machine, we have developed a water Cherenkov neutron detector (WCND) as a low-cost neutron detector. The system for detecting nuclear materials is composed of the neutron rotation machine and WCND, leading to a compact and low-cost. In previous studies, we accomplished to detect lead-shielded high enriched uranium (HEU) using the system [1]. However, in the experiments, the nuclear material was placed at the center of the measurement object. In actual nuclear material detection, nuclear material does not always exist at the center position, for example, nuclear material in a container. Therefore, in this experiment, we worked on the detection of nuclear material placed off-center.

****

EXPERIMENTS: The rotation machine can rotate the disk (32 cm in diameter), where a neutron source is installed at its outer periphery, at a rotation speed between 0 and 4000 rpm. A neutron source of Californium-252 whose reactivity was 1.3 MBq was set in the disk. The size of the WCND is 30x25x30 cm, with four 2 inch PMTs mounted on the ceiling. Polyethylene blocks were placed between the rotating irradiation device and the WCND, and a 20x20x20 cm space was provided inside the polyethylene blocks for measurement sample placement (Figure 1). To investigate the effect of placing the nuclear material away from the central position, the nuclear material was placed at the edge within the measurement space.

****

RESULTS: An example of the measurement results is shown in Figure 2. The measurement time was 10 minutes. By analyzing the spectrum, it was possible to determine the presence of nuclear materials placed at an edge within the measurement space. As a next step for our study, we are going to work on detection nuclear materials in various positions of the measurement space, and development of a more effective data processing method.

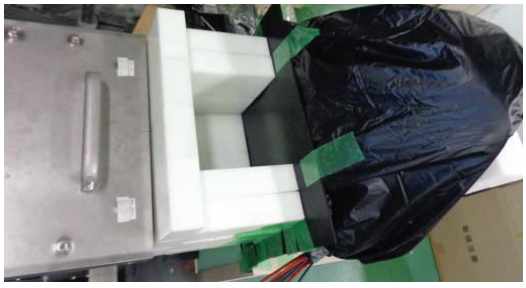

Fig. 1 The rotation machine (left), WCND (right), and sample placement area (middle). The lid is attached during measurement.

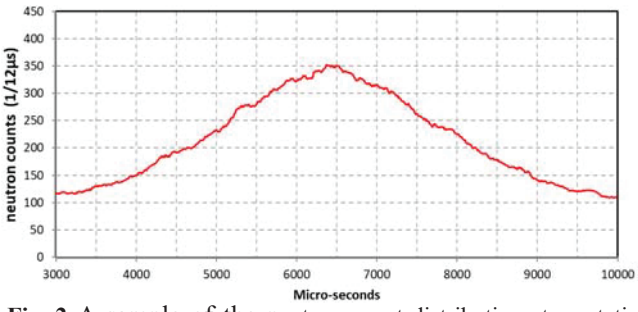

Fig. 2 A sample of the neutron count distribution at a rotation s eed of 4000 r m, in the resence of nuclear materials.

REFERENCES:

[1] K. Tanabe *et al.*, Scientific reports, **14** (2024) 18828.

CO8-2

New boron drug development research targeting pancreatic cancer

H. Michiue[1], T. Fujimoto[1,2], N. Kanehira[1,2], K. Igawa[1], Y. Sakurai[3], N. Kondo[3], T. Takata[3], and M. Suzuki[3]

[1]*Neutron Therapy Research Center, Okayama University; 2-5-1, Shikata-cho, Kita-ku, Okayama City, Okayama, Japan.*

[2]*Department of Gastroenterological Surgery, Okayama University; 2-5-1, Shikata-cho, Kita-ku, Okayama City, Okaya-ma, Japan.*

[3]*Institute for Integrated Radiation and Nuclear Science, Kyoto University, 2-1010, Asashiro-Nishi, Kumatori-cho, Sen-nan-gun, Osaka, Japan.*

INTRODUCTION: Pancreatic cancer refers to malignant tumors that originate in the pancreas, but it gener-ally refers to ductal cancer. Ductal cancer arises from the pancreatic duct epithelium and accounts for 80–90% of ma-lignant tumors in the pancreas. According to national statistics, it is the fifth leading cause of death, following lung cancer, stomach cancer, colorectal cancer, and liver cancer. In recent years, the number of pancreatic cancer patients in Japan has been increasing, with over 30,000 deaths annually.

Despite being a malignant tumor, pancreatic cancer has relatively fewer tumor vessels compared to normal tissue and exhibits interstitial hyperplasia between tumor cells, making it difficult for drugs to reach the tumor.

In the development of drugs for pancreatic cancer, the use of polymer-based DDS formulations with EPR effects (Enhanced Permeability and Retention effect) is considered challenging for future clinical applications. Therefore, we have decided to develop boron-based drugs targeting glucose transporters highly expressed in pancreatic cancer, using glucose as the basis.

****

EXPERIMENTS: In this study, we planned to develop boron-containing drugs targeting pancreatic cancer. Three cell lines were used: PANC0403 and BxPC3, which express high levels of CA19-9, and PANC-1, which express-es low levels of CA19-9. The drugs used were three types of boron-containing agents: glucose-bound BSH, BPA, and BSH. After evaluating the cellular uptake of the drugs, neutron irradiation was performed using a reactor neutron source.

****

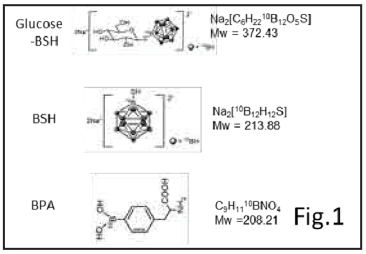

Fig.1

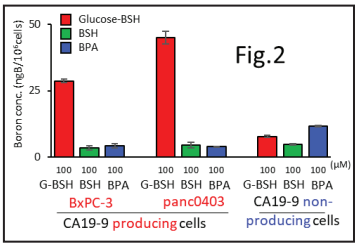

Fig.2

RESULTS:

Ex1) The three boron drugs used in this study were Glucose-BSH (G-BSH), BSH, and BPA, with molecular weights of 372.43, 213.88, and 208.21, re-spectively, and intramolecular boron contents of 0.322, 0.561, and 0.048 ngB, respectively (Fig.1). We treated three pancreatic cell lines, panc0403 and BxPC3 CA19-9-producing cells and PANC-1 CA19-9-non-producing cells with the boron drugs and examined intracellular boron concentrations (Fig. 2). All three cell lines, both CA19-9-producing and CA19-9-non-producing cells, showed low intracellular boron concentrations after treatment with BSH and BPA. In contrast, very high intracellular boron concentrations in the G-BSH group were observed in the panc0403 and BxPC3 CA19-9-producing cells, while low concentrations were ob-served in the PANC-1 CA19-9-non-producing cells (Fig. 2).

Ex2) We next performed colony formation assays in CA19-9-producing PC cells panc0403 and non-CA19-9-producing PANC-1 cells treated with boron agents and irradiated with neutrons. In panc0403 cells, Glucose-BSH showed superior inhibition of cell proliferation compared with the Control, BPA, and BSH treatments starting from 30 min of irradia-tion and 45 min (P>0.001). In contrast, none of the boron agents showed significant cell-killing effects in CA19-9-non-producing PANC-1 cells (BPA: P>0.4, BSH: P>0.6) (Fig. 3). Treatment doses were as high as 19.1, 34.9, and 53.2 Gy-Eq each in the Glucose-BSH group of panc0403 cells for 15, 30, and 45 min of irradiation, respectively; the Glucose-BSH group showed 5-fold higher neutron doses than the BPA and BSH groups. These results indicate that Glucose-BSH showed strong cytotoxic activ-ity against CA19-9-producing pancreatic cancer cells upon neutron ir-radiation.

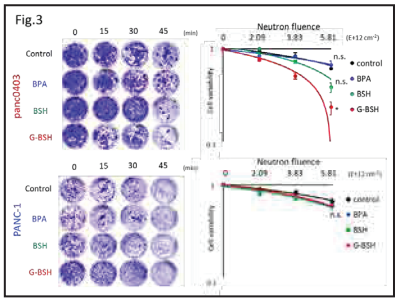

****

REFERENCE: [1] T. Fujimoto *et al.,* Biomaterials, **309** (2024) 122605.

CO8-3

Porocity Distribution Evaluation of Additively Manufactured Workpiece Using Neutron Phase Imaging

Y. Kanbe, Y. Terakawa[1], Y. Seki[1], D. Kono, M. Hino[2]

Graduate School of Engineering, Department of Microengineering, Kyoto University
[1]Institute of Multidisciplinary Research for Advanced Materials, Tohoku University
[2]Institute for Integrated Radiation and Nuclear Science, Kyoto University

INTRODUCTION: Since the porosity distribution in additively manufactured workpiece is highly variable, it is necessary to inspect the porosity distribution to assure the quality of the workpiece. In this study, we investigated the potential of neutron phase imaging as a non-destructive inspection method for porosity distribution. The porosity of samples were measured by the neutron phase imaging and the conventional microscope observation for comparison.

EXPERIMENTS: Samples were prepared by changing fabrication parameters that are laser power, scanning speed, and rotation angle of scanning specifically. The porosity of samples was measured by the neutron phase imaging based on the rigid sphere model proposed by Strobl et al.. The porosity was also measured from the cross sectional image of samples taken by a digital microscope. Samples were cut, embedded into plastic pellets, and polished for observation. The cross sectional image was binarized to extract the pore area. Then, the area ratio of pores relative to the matrix was calculated as porosity.

RESULTS: Figure 1 shows the obtained visibility image of samples. The variation of the porosity depending on the fabrication conditions can be observed from the visibility image. Some samples such as sample 4, 7, 16, and 17 have laminar structured image that indicates the corresponding periodic porosity variation. The porosity measured by the neutron phase imaging had a positive correlation with porosity measured by the microscope. However, the difference of the absolute porosity was up to 20 % and not negligible. The reason for this discrepancy may be the influence of pores with the size larger than the auto correlation length in the neutron phase imaging.

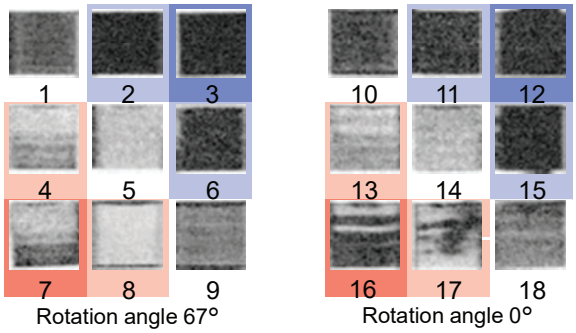

Fig. 1. Visibility image of samples fabricated by different conditions. Black and white colors represent higher and lower porosities, respectively.

REFERENCES:

[1] M. Strobl, Scientific Reports, **4** (2014) 7243.